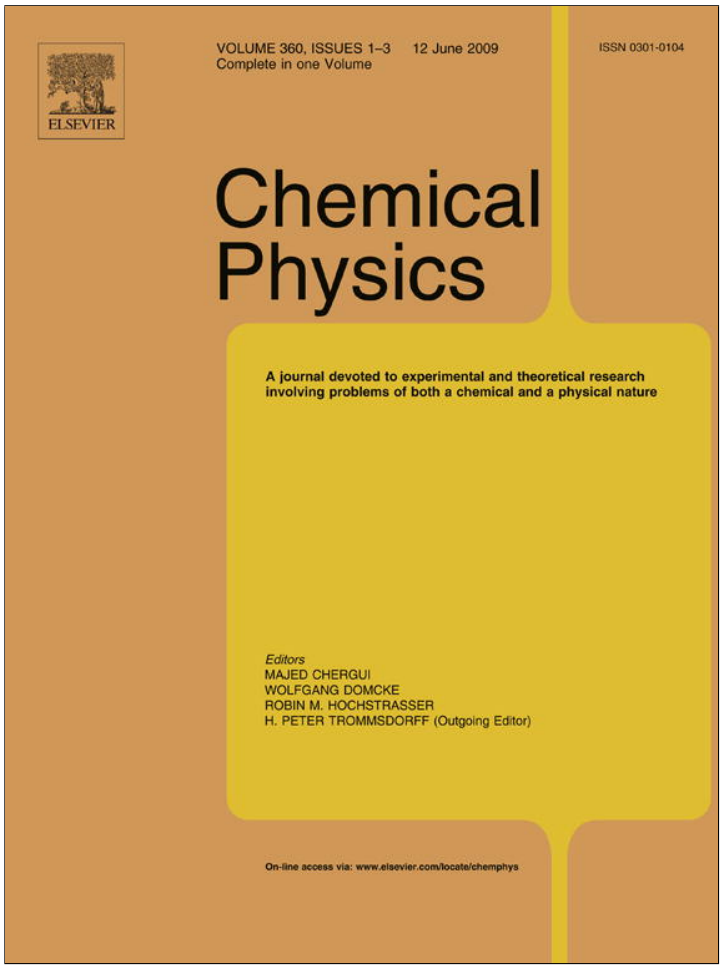

Chemical Physics 360 (2009) 171–175

Contents lists available at ScienceDirect

Chemical Physics

journal homepage: www.elsevier.com/locate/chemphys

The mechanism of nitrogen fluorescence inside a femtosecond laser filament in air

H.L. Xu *, A. Azarm, J. Bernhardt, Y. Kamali, S.L. Chin

Department of Physics, Center of Optics Photonics and Laser (COPL), Université Laval, Québec City, Québec, Canada G1V 0A6

ARTICLE INFO

Article history:
Received 10 May 2008
Accepted 1 May 2009
Available online 6 May 2009

Keywords:
Filamentation
Air
Fluorescence

ABSTRACT

The visible and near-UV fluorescence spectroscopy of air generated inside a femtosecond laser plasma filament was studied. The primary reactions, $N_2^+ + N_2 \Rightarrow N_4^+; N_4^+ + e \Rightarrow N_2(C^3\Pi_u) + N_2$, populates the electronic excited state $N_2(C^3\Pi_u)$ of N_2. The N_2 fluorescence is not by direct electron–ion recombination of $N_2^+ + e$. Using a pump–probe method, the fluorescence lifetime of $C^3\Pi_u$ of N_2 at atmospheric pressure was determined to be about 85 ps.

1. Introduction

Filamentation generated by high-power, ultrafast laser pulses in the atmosphere has attracted a lot of interest in recent years because of its promising applications in areas such as remote sensing of chemical/biological agents, generation of few cycle pulses and lightning control [1–8]. The formation of femtosecond laser filamentation is by now well understood. Filaments appear as a result of a dynamic interplay between self-focusing and defocusing of plasma produced by multiphoton/tunnel ionization of air molecules. This balance gives the laser intensity inside the filament core of about 5×10^{13} W/cm^2 (intensity clamping), and creates a long but weak plasma column along the femtosecond laser pulse propagation [9,10]. It has been shown that the plasma filament can persist over several tens of meters [11,12], and its formation has been observed as far as a few kilometers in the atmosphere [13].

The properties of the plasma filament such as the density, lifetime, temperature and diameter have been extensively investigated in order to improve/optimize the efficiency of many nonlinear physical/chemical processes (see e.g. Ref. [3] and the references therein). To characterize the plasma filament, one method is to utilize the fluorescence emission from the air molecules induced by the filamentation. For instance, Théberge et al. have experimentally demonstrated that the plasma density and diameter are strongly dependent on the external focusing based upon side imaging of the nitrogen fluorescence and longitudinal diffraction techniques [14]. Arevalo and Becker have numerically analyzed the role of the combined effect of self-focusing, geometrical focusing and plasma defocusing in the formation of the fluorescence signal during the filamentation of an ultrashort laser pulse in nitrogen molecular gas [15]. Luo et al. have presented that the fluorescence emission can be used to provide information on parameters such as the position and length of the plasma filament [16]. Therefore, there is a necessity to study the spectroscopy of the plasma filament in terms of the fluorescing mechanisms of different species.

The fluorescence emission from the plasma filament is very clean [17], which is in contrast to those obtained by electron impact or laser breakdown (see e.g. Ref. [18] and references therein). Previously, the fluorescence from the first negative band system ($B^2\Sigma_u^+ - X^2\Sigma_g^+$transition) of N_2^+ in the plasma filament has been studied, which results from intense laser-induced multiphoton or tunnel ionization of inner-valence electrons of neutral nitrogen molecules, leaving the molecular ion N_2^+ in the excited state $B^2\Sigma_u^+$ [19]. However, after the formation of the plasma filament, the information on the chemical reactions of difference species inside the weakly ionized plasma is, so far, not fully clear. In this work, we study the mechanism of generating visible and near-UV fluorescence spectra of air generated inside a femtosecond laser filament. It is found that the primary reaction $N_2^+ + N_2 = N_4^+$ followed by the recombination with the electron is responsible for populating the electronic excited state $C^3\Pi_u$ of N_2. The N_2 fluorescence is not by direct electron–ion recombination of $N_2^+ + e$. Using a pump–probe method, the lifetime of $C^3\Pi_u$ of N_2 is determined.

2. Experimental set-up

The experiments were conducted using a Ti:Sapphire femtosecond laser system. The laser pulses, emitted from a Ti:Sapphire oscillator (Spectra Physics Tsunami), were positively chirped to

* Corresponding author. Address: Department of Chemistry, The University of Tokyo, 7-3-1 Hongo, Bunkyo-ku, Tokyo 113-0033, Japan.
E-mail addresses: huailiang.xu.1@ulaval.ca, hlxu@chem.s.u-tokyo.ac.jp, huailiang.xu@gmail.com (H.L. Xu).

0301-0104/$ - see front matter © 2009 Elsevier B.V. All rights reserved.
doi:10.1016/j.chemphys.2009.05.001

about 200 ps in a stretcher and amplified in a regenerative amplifier (Spectra Physics Spitfire). The pulses with a repetition rate of 1 kHz were further amplified in a two-pass Ti:Sapphire amplifier and then compressed to about 40 fs. The pulse spectrum had a central wavelength at 800 nm. The energy per pulse was 2 mJ and the beam radius was about 3 mm (1/e level of intensity). The laser beam was focused into air at ambient pressure using a fused-silica lens (f = 100 cm, thickness = 2 mm). The focused pulse propagated in air and created a stable plasma single filament, which was confirmed by the observation of a single hot spot on a burn paper. The filament had a length of about 5 cm, terminating at the position of the focal point of the lens. The induced fluorescence was collected at a right angle to the filament and then focused into a spectrometer (Acton Research Corp., SpectraPro-500i), equipped with a gated intensified charge coupled device (ICCD, Princeton instruments Pi-Max 512). The entrance slit of the spectrometer was arranged to be parallel to the plasma filament in order to increase the fluorescence collection efficiency. A pump–probe apparatus was also built in order to study the time evolution of the fluorescence emission from the plasma filament. In the pump–probe setup, the laser beam was split into two parts by a 50/50 splitter. One arm of the beam with the energy of about 850 μJ was focused by a fused-silica lens (f = 30 cm) to generate the plasma filament. The other arm of the beam passed through a delay stage, a half-wave plate and a KDP crystal. The generated second harmonic (the probe pulse) was reflected by two dichroic mirrors and then spatially overlapped with the plasma filament. The probe pulse energy was about 25 μJ. The variation of fluorescence intensity was monitored by a photomultiplier tube (PMT, Hamamatsu R1464), which was connected to an oscilloscope (Tektronix, TDS3054B).

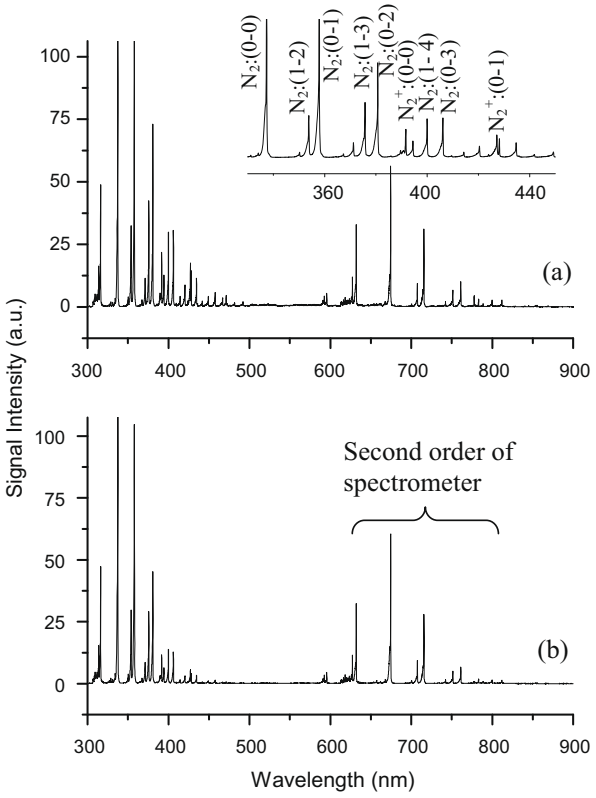

Fig. 1. Fluorescence spectrum of a plasma filament induced by (a) linearly or (b) circularly polarized femtosecond intense laser pulses at atmospheric pressure. The artificial bands in Fig. 1a observed in the range of 600–900 are due to the second order of the spectrometer. The inset shows a part of the spectrum in a higher resolution.

3. Results and discussion

Fig. 1 shows the femtosecond laser-induced fluorescence spectrum of air obtained in the ambient atmosphere in the range of 200–900 nm. The data were averaged over 5000 shots. The ICCD gate width was set to 20 ns and the gate was opened 3 ns before the laser pulse arrived at the interaction zone. It can be seen from Fig. 1a that the fluorescence emission from the plasma filament is very "clean", i.e., the contribution of continuum emission to the spectrum is negligible, which agrees well with previous observation [17]. The inset of Fig. 1a shows the spectrum in a higher resolution in the range of 300–500 nm. The spectral bands have been assigned to the first negative band system of $N_2^+(B^2\Sigma_u^+ - X^2\Sigma_g^+$ transition) and the second positive band system of $N_2(C^3\Pi_u - B^3\Pi_g$ transition) [17]. The numbers in the parentheses $(v - v')$ denote the vibrational levels of the upper and the lower electronic states. It has been previously demonstrated that the emission from the $B^2\Sigma_u^+$ state of N_2^+ results from laser-induced multiphoton or tunnel ionization of inner-valence electrons of neutral nitrogen molecules [19]. But the mechanism by which the excited state $C^3\Pi_u$ of N_2 is populated inside the plasma filament is still unclear. Here we attempt to answer this question.

There are three possible mechanisms to populate the excited state $C^3\Pi_u$ of N_2. One is by direct excitation of laser light; the second is by the excitation of inelastic electron collision; and the third is by electron–ion recombination. We first exclude the direct excitation of the $C^3\Pi_u$ state by laser light because the transition between the ground electronic state $X^1\Sigma_g^+$ and the triplet electronic state is forbidden. We also conclude that the excitation of $C^3\Pi_u$ by inelastic electron collision is highly unlikely. This can be explained from three aspects as follows. Firstly, it is known that in the re-collision theory of intense laser fields, the electron accelerated by the laser field will re-scatter back to its parent molecule. Taking into account the clamped laser intensity, 5×10^{13} W/cm^2, inside the filament core, the ponderomotive energy [20], U_p, amounts to 3 eV and most of electrons have the energy less than 3.2 U_p = 9.6 eV, which however is not enough to excite the state $C^3\Pi_u$ of N_2 (~14.1 eV for the maximum cross section of $C^3\Pi_u$ by electron impact [21]). Furthermore, we also measured the fluorescence spectrum of air inside the plasma filaments induced by circularly polarized femtosecond laser pulses, as shown in Fig. 1b. The fluorescence bands emitted from the $C^3\Pi_u$ state of N_2 can be clearly observed. Since the process that the electron re-scatters back to its parent core, which has a total energy of 3.2 Up + IP, is very susceptible to the laser polarization, the direct excitation of the parent core by the re-scattering electron would not be the main mechanism for populating the $C^3\Pi_u$ state of N_2. Secondly, when the plasma is in the case of local thermodynamic equilibrium, the electrons with the electron temperature of $T_e \approx 5800$ K [22] in the plasma filament will only have an averaged kinetic energy of less than 1 eV. The electron with this energy does not have the chance to further absorb the energy from the laser photons (this process will take about 350 fs in air [23]) within the duration of the laser pulse used here (~40 fs). Thirdly, the excitation of $C^3\Pi_u$ by inelastic electron collision would depend linearly on the pressure, which disagrees with the experimental observation of quadratic pressure dependence, as shown in Ref. [17]. As a result, we exclude the second mechanism. This gives rise to a remarkably different consequence from that obtained from the electron impact or long-pulse laser breakdown experiments, where the population of the excited state $C^3\Pi_u$ of N_2 could be ascribed to the inelastic collision excitation by energetic electrons.

Next, we consider the possibility to populate the $C^3\Pi_u$ state by electron–ion recombination. It should be pointed out that the

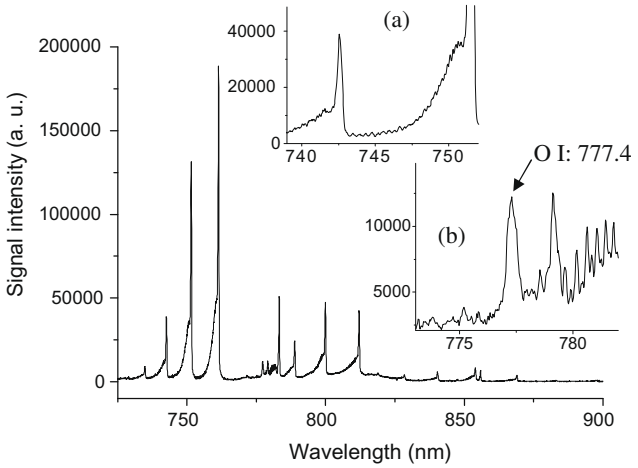

Fig. 2. Fluorescence spectrum in the range of 725–900 nm with a 10 times amplification as shown in Fig. 1. The insets show parts of the spectrum in a higher resolution. No atomic nitrogen line at 746.8 nm, but a very weak atomic oxygen line at 777.4 nm can be observed.

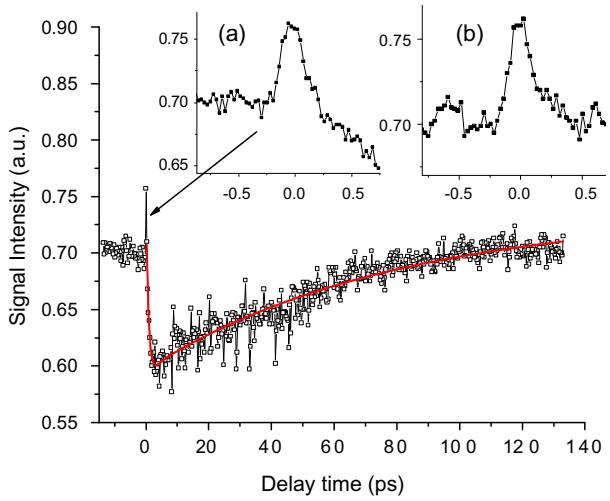

Fig. 3. Fluorescence emission from the $C^3\Pi_u$ state at 337 nm as a function of the delay time between the pump and probe beams. The solid line represents the fit curve with the rate equation for the dynamics of the $C^3\Pi_u$ state (see text). The inset (a) shows the same data but in a higher resolution, and the inset (b) shows the fluorescence signal from the $B^2\Sigma_u^+$ state of N_2^+ at 391 nm as a function of the delay time.

direct recombination of $N_2^+ + e$ would not contribute to the yield of $N_2(C^3\Pi_u)$ because the energy released in the recombination breaks the chemical bond of N–N through an intramolecular *E–V* energy transfer process, leading to $e + N_2^+ \Rightarrow N^* + N$ [24]. In particular, as can be seen in Fig. 2, no atomic N is observed (i.e., the absence of the strongest expected line of atomic nitrogen at 746.83 nm as shown in the inset (a) of Fig. 2). This implies that in our experiment the dissociative recombination of $e + N_2^+$ does not dominate the depletion of N_2^+ in the plasma. Therefore, the picture for the recombination regarding N_2^+ gets much simpler in our case, because those reactions involved in the plasma by electron excitation and direct dissociative recombination of $e + N_2^+$ are negligible [25]. Notice that at a relatively high pressure (a few Torr) the main positive constituent nitrogen in the plasma is expected to be N_4^+ in discharge experiments [26–28], and that our experiment was conducted at atmospheric pressure, so that we conclude that the dissociative recombination through the N_4^+ formation ($N_2^+ + N_2 \Rightarrow N_4^+; N_4^+ + e \Rightarrow N_2(C^3\Pi_u) + N_2$) is a dominant process for populating the $C^3\Pi_u$ state. This is also supported by the fact that there is a very low concentration ratio of N_2^+/N_2 inside the plasma filament (the electron density of filament-induced plasma is around $10^{16}/cm^3$, i.e., the number density of the ionized molecules is around $10^{16}/cm^3$, 80% of the ions in the femtosecond induced plasma filament are due to the oxygen molecules [10], and the number density of air is about $2.5 \times 10^{19}/cm^3$), and that the reaction rate of $N_4^+ + e \Rightarrow N_2(C^3\Pi_u) + N_2$ in the processes involved in the plasma is highest. As a consequence, although it has been shown that the picture for electron–ion recombination in the plasma of nitrogen–oxygen mixtures produced by LIBS and electron impact is quite complicated [25], the recombination processes regarding N_2^+ in a plasma filament induced by femtosecond intense laser pulses is simply through the reaction path of $N_2^+ + N_2 \Rightarrow N_4^+; N_4^+ + e \Rightarrow N_2(C^3\Pi_u) + N_2$.

To explore the decay property of the $C^3\Pi_u$ state, we measured, using a pump–probe method, the integrated fluorescence emission from the $C^3\Pi_u$ state at 337 nm as a function of the delay time between the pump and probe beams. It was expected that after the plasma was created, the application of the second laser pulse would kick off the electron from the $C^3\Pi_u$ state of N_2 (two-photon process with the probe pulse at 400 nm), giving rise to a decrease of the total fluorescence emission. Therefore, by plotting the integrated fluorescence signal as a function of the delay time between the pump and probe beams, the decay profile of the $C^3\Pi_u$ state could be obtained. As expected, in Fig. 3, a relatively slow decay profile can be clearly observed, but an enhancement of the fluorescence signal at the delay time of $t = 0$ also occurs (see the inset (a) of Fig. 3) (Note that the zero line in Fig. 3 represents the signal intensity obtained only with the pump beam.). To understand this enhancement, the fluorescence emission from the $B^2\Sigma_u^+$ state of N_2^+ at 391 nm was also measured as a function of the delay time, as shown in the inset (b) of Fig. 3. A significant increase of the fluorescence signal can be observed, which resembles to the inset (a) of Fig. 3. This behavior could be considered as an ionization enhancement of N_2^+ when the pump and probe pulses were temporally overlapped. The ionization enhancement of N_2^+ will further lead to an increase of the excited N_2.

As already pointed out, the excited states are dominantly populated by the dissociative recombination through the N_4^+ formation ($N_2^+ + N_2 \Rightarrow N_4^+; N_4^+ + e \Rightarrow N_2(C^3\Pi_u) + N_2$). The dynamics of such reactions can be described by the following rate equations:

$$d[N_4^+] = -k_1[N_4^+] + R_1[N_2^+][N_2] \quad (1)$$

$$d[N_2^*] = -k_2[N_2(C^3\Pi_u)] + R_2[N_4^+][\text{electron}] \quad (2)$$

where $[x]$ refers to the population/density of species x, k_1 and k_2 the spontaneous decay rates of N_4^+ and $N_2(C^3\Pi_u)$, R_1 and R_2 the rates of the reactions $N_2^+ + N_2 \Rightarrow N_4^+$ and $N_4^+ + e \Rightarrow N_2(C^3\Pi_u) + N_2$. Here it is reasonable to assume that $[N_2]$ is constant and $[N_2^+]$ and [electron] decay exponentially with a rate of k_3 and k_4. Finally, the solution of $[N_2(C^3\Pi_u)]$,

$$[N_2(C^3\Pi_u)](t) = D_1\exp(-k_2t) + D_2\exp(-(k_3+k_4)t) + D_3\exp(-(k_1+k_4)t) \quad (3)$$

was used to fit the experimental data in Fig. 3. The lifetimes obtained are 85 ± 15, 1.2 ± 0.6 and 1.1 ± 0.6 ps, respectively. The large errors for these two short decays originate from the fact that the enhancement at the delay time of $t = 0$ has distorted the rising part of the decay curve with an error of about 150 fs. We assigned the relatively long decay of 85 ps as the fluorescence lifetime of the $C^3\Pi_u$ state of N_2. It should be pointed out that this value (85 ps) is much shorter than the fluorescence lifetime of the $C^3\Pi_u$ state measured in pure nitrogen at atmospheric pressure (about 1–2 ns). In order to check the reliability of the value (85 ps), we measured the fluorescence lifetime of the $C^3\Pi_u$ state of N_2 at a pressure of

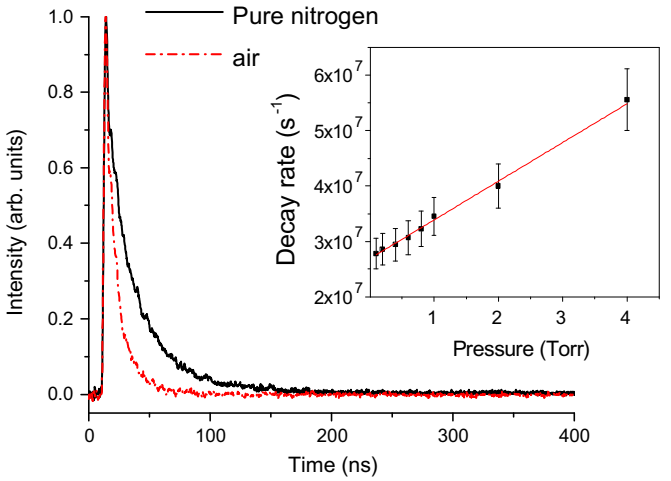

Fig. 4. Fluorescence decays of the excited state $C^3\Pi_u$ of N_2 in air (dash line) and in pure nitrogen (solid line) with the pressure of 20 Torr for both cases. The decay curves were obtained by monitoring the $C^3\Pi_u$–$B^3\Pi_g$ (0–0) transition of N_2 at 337 nm. In the inset, the decay rate of the $C^3\Pi_u$ state of N_2 measured as a function of pressure together with its linear fit (solid line) is shown.

4 Torr in pure nitrogen, as well as in air, as shown in Fig. 4. It can be seen that the decay time of the $C^3\Pi_u$ state of N_2 in air is much shorter than that in pure nitrogen. This discrepancy might be due to the quenching mechanism of the excited state of N_2 in air different from that in pure nitrogen. We also measured the decay curves of the $C^3\Pi_u$ state of N_2 in air at different pressures and plotted the decay rate of the $C^3\Pi_u$ state of N_2 as a function of pressure (the inset of Fig. 4), from which, by extrapolation, the radiative lifetime of the $C^3\Pi_u$ state of N_2 (at zero pressure) is obtained to be about 37 ns and the fluorescence lifetime of this state at atmospheric pressure to be about 200 ps. This value of 200 ps is in agreement with the result obtained directly by the pump–probe measurements, indicating that the quenching mechanism of air is different from that of pure nitrogen.

There is a difficulty to assign those two very short decays. However, since it has been previously shown that the plasma can persist for tens of nanoseconds [29,30], the decay rate k_4 of [electron] would be much smaller, compared to k_1, k_3, thus $k_1 + k_4 \approx k_1$ and $k_3 + k_4 \approx k_3$. As a consequence, although the errors for the lifetimes obtained for N_2^+ and N_4^+ are very large, they provide information on the temporal evolution of N_2^+ and N_4^+ with a magnitude of the order of 1–2 ps in the plasma filament. The mechanism for the fast collisional process is still not totally clear, but it might be due to the following scenario. The mean collision time is determined by two factors, i.e., the velocity of the randomly moving molecules and the mean free path. The mean collision time of nitrogen molecules at STP is ~130 ps (the mean free path, l, is ~65 nm and the averaged velocity of nitrogen molecules, v_0, is ~500 m/s at STP [31,32]). As measured in Ref. [17], the averaged electron temperature in the plasma filament is about 5800 K, giving rise to an increase of the average velocity of nitrogen molecules from v_0 to $(5800/273)^{1/2} v_0 \sim 4.6\ v_0$. Therefore, the contribution of the temperature will decrease the mean collision time from ~130 ps to ~35 ps if the mean free path, l, keeps constant. It is known that the mean free path can be expressed as $l \propto 1/\sigma n_v$, where σ is the collision cross section and n_v is the molecule number per unit volume. Since in the very short time of <5 ps, the molecule number per unit volume inside the plasma filament could be considered to be constant, the mean free path is thus determined only by the collision cross section. In our case, the intense laser fields can induce nonlinear electric dipole moments in the nitrogen molecules/molecular ions by, for instance, inducing an 'instantaneous' nonlinear polarization of the gas. This latter is recently observed in what is called ultrafast birefringence inside a gas filament [33,34]. The collision cross section for the collisions between both the polarized N_2^+ and N_2 having nonlinear electric dipole moments inside the focal volume should be much larger than that for the collisions between two unaffected neutral nitrogen molecules at STP; this decreases the mean collision time. Therefore, the formation of N_4^+ may mainly result from the collisions between the molecular ion of N_2^+ and its neighboring nitrogen molecule whose nonlinear electric dipole moments are not zero.

4. Conclusion

The visible and near-UV fluorescence spectra of air generated inside femtosecond laser filament was presented. It is found that the N_2^+ ion is dominantly depleted by the formation of $N_4^+ (N_2^+ + N_2 = N_4^+)$, and the dissociative recombination of $N_4^+ + e$ is responsible for populating the electronic excited state $C^3\Pi_u$ of N_2. Using a pump–probe method, the decay times of these species have been determined to be in the range of sub-picoseconds and picoseconds.

Acknowledgments

We thank G. Méjean and W. Liu for discussions regarding this work and F. Théberge for his assistant in the laboratory during the preparation of the pump–probe setup. The support by Q. Liu and M. Sarifi in the early part of this work is acknowledged. This work was partially supported by NSERC, DRDC Valcartier, Canada Research Chairs, CIPI, CFI, Femtotech, FQRNT and the Global COE program.

References

[1] S.L. Chin, Phys. Can. 60 (2004) 273.
[2] S.L. Chin, S.A. Hosseini, W. Liu, Q. Luo, F. Théberge, N. Aközbek, A. Becker, V. Kandidov, O. Kosareva, H. Schröder, Can. J. Phys. 83 (2005) 863.
[3] A. Couairon, A. Mysyrowicz, Phys. Rep. 441 (2007) 47.
[4] H.L. Xu, J.F. Daigle, Q. Luo, S.L. Chin, Appl. Phys. B 82 (2006) 655.
[5] J.-F. Daigle, G. Méjean, W. Liu, F. Théberge, H.L. Xu, Y. Kamali, J. Bernhardt, A. Azarm, Q. Sun, P. Mathieu, G. Roy, J.-R. Simard, S.L. Chin, Appl. Phys. B 87 (2007) 749.
[6] H.L. Xu, W. Liu, S.L. Chin, Opt. lett. 31 (2006) 1540.
[7] W. Liu, H.L. Xu, G. Méjean, Y. Kamali, J.-F. Daigle, A. Azarm, P.T. Simard, S.L. Chin, P. Mathieu, Spectrochim. Acta Part B 62 (2007) 76.
[8] H.L. Xu, Y. Kamali, C. Marceau, P.T. Simard, W. Liu, J. Bernhardt, G. Méjean, P. Mathieu, G. Roy, J.-R. Simard, S.L. Chin, Appl. Phys. Lett. 90 (2007) 101106.
[9] H.R. Lange, A. Chiron, J.-F. Ripoche, A. Mysyrowicz, P. Breger, P. Agostini, Phys. Rev. Lett. 81 (1998) 1611.
[10] J. Kasparian, R. Sauerbrey, S.L. Chin, Appl. Phys. B 71 (2000) 877.
[11] G. Méchain, C. D'Amico, Y.-B. André, S. Tzortzakis, M. Franco, B. Prade, A. Mysyrowicz, A. Couairon, E. Salmon, R. Sauerbrey, Opt. Commun. 247 (2005) 171.
[12] A. Brodeur, C.Y. Chien, F.A. Ilkov, S.L. Chin, O.G. Kosareva, V.P. Kandidov, Opt. Lett. 22 (1997) 304.
[13] M. Rodriguez, R. Bourayou, G. Méjean, J. Kasparian, J. Yu, E. Salmon, A. Scholz, B. Stecklum, J. Eislöffel, U. Laux, A.P. Hatzes, R. Sauerbrey, L. Wöste, J.-P. Wolf, Phys. Rev. E 69 (2004) 036607.
[14] F. Théberge, W. Liu, P.Tr. Simard, A. Becker, S.L. Chin, Phys. Rev. E 74 (2006) 036406.
[15] E. Arévalo, A. Becker, Phys. Rev. A 72 (2005) 043807.
[16] Q. Luo, S.A. Hosseini, B. Ferland, S.L. Chin, Opt. Commun. 233 (2004) 411.
[17] A. Talebpour, M. Abdel-Fattah, A.D. Bandrauk, S.L. Chin, Laser Phys. 11 (2001) 68.
[18] F. Martin, R. Mawassi, F. Vidal, I. Gallimberti, D. Comtois, H. Pépin, J.C. Kieffer, H.P. Mercure, Appl. Spectrosc. 56 (2002) 1444.
[19] A. Becker, A.D. Bandrauk, S.L. Chin, Chem. Phys. Lett. 343 (2001) 345.
[20] E. Constant, E. Mevel, in: C. Rulliere (Ed.), Femtosecond Laser Pulses: Principles and Experiments, Springer, New York, 2005, p. 395.
[21] M. Zubek, J. Phys. B 27 (1994) 573.
[22] J. Bernhardt, W. Liu, F. Théberge, H.L. Xu, J.F. Daigle, M. Châteauneuf, J. Dubois, S.L. Chin, Opt. Commun. 281 (2008) 1268.
[23] M. Mlejnek, E.M. Wright, J.V. Moloney, IEEE J. Quant. Electron. 35 (1999) 1771.
[24] J.N. Bardsley, J. Phys. B 1 (1968) 365.

[25] I.A. Kossyi, A.Yu. Kostinsky, A.A. Matveyev, V.P. Silakov, Plasma Sources Sci. Technol. 1 (1992) 207.
[26] W.H. Kasner, M.A. Biondi, Phys. Rev. 137 (1965) 317.
[27] D.H. Hamilton, J. Chem. Phys. 58 (1973) 4820.
[28] R.F. Boivin, E.E. Scime, Plasma Sources Sci. Technol. 14 (2005) 283.
[29] S. Tzortzakis, M. Franco, B. Prade, A. Mysyrowicz, Opt. Commun. 181 (2000) 123.
[30] H.D. Ladouceur, A.P. Baronavski, D. Lohrmann, P.W. Grounds, P.G. Girardi, Opt. Commun. 189 (2001) 107.
[31] S.G. Jennings, J. Aerosol Sci. 19 (1988) 159.
[32] R.K. Hobbie, Intermediate Physics for Medicine and Biology, third ed., Springer, 1997, p. 83.
[33] P. Béjot, Y. Petit, L. Bonacina, J. Kasparian, M. Moret, J.-P. Wolf, Opt. Exp. 16 (2008) 7564.
[34] Y. Chen, C. Marceau, F. Théberge, M. Châteauneuf, J. Dubois, S.L. Chin, Opt. Lett. 33 (2008) 2731.